

Wind-driven Rain Simulations

Hangan, H.*

* The Boundary Layer Wind Tunnel Laboratory, Faculty of Engineering Science, University of Western Ontario, London, Ontario, N6A 5B9, Canada.

Received 29 July 1998.
Revised 17 February 1999.

Abstract: Wind-driven rain studies provide the main input to problems such as: precipitation protection, sealing, drainage accumulation. A Computational Fluid Dynamics (CFD) methodology is developed and used to compute trajectories and local intensity factors for two generic buildings, previously tested in the wind tunnel. The methodology is further applied in investigating real problems such as the role played by cornice in protecting the upper part of a low-rise building or the wetting and downwash on a sloped face of a high-rise building.

Keywords: wind-driven rain, computational fluid dynamics, wind tunnel, particle trajectories.

1. Introduction

Water damage to wall systems and interiors of buildings is a continuing problem in construction. The problem is complex: wind-driven rain impacts a building non-uniformly and differentially depending on the speed of the wind, the intensity of the rain and the geometry of the building. The objective of the present study is to develop a numeric methodology for the prediction of wetting patterns and associated water quantities impacting generic building geometries in realistic wind flows, to compare the CFD results with wind tunnel experiments and to apply the technique to real buildings.

2. Modeling

Many components of the methodology already exist; however, they have not been brought together in a form for general application, nor have they been thoroughly tested. The basis of the computational method is the FLUENT commercial CFD package (1996), to which suitable models of rain are added, based on data existing in the literature. Physical models of wind-rain effects on building have been previously developed at the BLWTL, and the wind tunnel experiments form the basis for the verification.

The modeling problem consists in calculating the raindrop trajectories in the presence of the air flow around the building. This is a Lagrangian approach and implies assumptions such as: low volume fraction of water in air (<10%) and neglect of particle-particle interaction.

The numerical process simulates the air flow around the building, calculates the raindrop trajectories, evaluates the coupling between the two phases (air-water) and reiterates. Finally the rainfall rates through various zones of the building facade are computed.

2.1 Wind Flow around Buildings

The flow field is solved using the Navier-Stokes (N-S) and continuity equations:

$$\frac{\partial u_i}{\partial t} + \frac{\partial}{\partial x_j} (u_i u_j) = -\frac{1}{\rho} \frac{\partial p}{\partial x_i} + \frac{\partial}{\partial x_j} \nu \left(\frac{\partial u_i}{\partial x_j} + \frac{\partial u_j}{\partial x_i} \right) \text{ (N-S)}; \frac{\partial u_i}{\partial x_i} = 0 \text{ (continuity)} \quad (1)$$

Both k - ε and Reynolds stress turbulence models are employed for the Eulerian (fluid phase) flow. These turbulence models are well documented in literature and will not be investigated here. Generally both physical (wind tunnel) and numerical simulations show typical wind flow patterns around buildings such as frontal base vortex, separation and reattachment, vortex shedding. The particles (especially the light ones) will have the tendency to follow the characteristic streamlines. Figure 1 shows typical particle trajectories for the high-rise building and Figure 2 shows particle trajectories for the low-rise generic building.

2.2 Wind-driven Rain

The raindrops are considered spherical of diameter d and density ρ_p and their terminal velocity is expressed based on the equilibrium between gravity and aerodynamic drag (Stokes formula) on the particle (2). The particles size distribution is expressed by a Gaussian (3).

$$V_T = \frac{d^2}{18\nu} \left(\frac{\rho_p - \rho}{\rho} \right) g \quad (2)$$

where ρ and ν are the air density and viscosity

$$M_d = \exp\left[-\left(\frac{d}{\bar{d}}\right)^n\right] \text{ the mass fraction of droplets larger than } d \quad (3)$$

where $\bar{d} = bR_0^n$ = a mean diameter, n a spread parameter ($n = 2.25$ for raindrops), R_0 (mm/hr) the undisturbed rainfall intensity, $b = 1.3$ and $p = 0.232$ (full scale values, Best 1950).

Raindrops trajectories are determined based on a force balance (Lagrangian reference) which equates the particle inertia ($\rho_p \frac{du_p}{dt}$) with forces acting on the particle such as the aerodynamic drag (F_D) and the gravitation (G) (4).

$$\rho_p \frac{du_p}{dt} = F_D(u_i - u_p) + g(\rho_p - \rho) \quad (4)$$

where u_i and u_p are the air and particle velocities, $F_D = \frac{18\nu\rho_p}{d^2} * \frac{C_D * \text{Re}}{24}$ is the aerodynamic drag (Stokes law), $\text{Re} = \frac{d}{\nu} \sqrt{\Sigma(u_i - u_p)^2}$ the particle Reynolds number (Lagrangian) and $C_D = a_1 + \frac{a_2}{\text{Re}} + \frac{a_3}{\text{Re}^2}$ is the drag coefficient (Morsi-Alexander law).

The turbulent dispersion of droplets is an important factor to be taken into consideration for flows around bluff bodies, such as buildings. This is achieved by integrating the trajectory equations using the instantaneous fluid velocity: $u = \bar{u} + u'$. The Discrete Random Walk model assumes that the particle interacts with a succession of discrete air turbulent eddies which are characterized by random velocity fluctuations $u' = v' = w' = \zeta \tilde{u}' = \sqrt{\frac{2k}{3}}$ time scales $\tau_e \sim \frac{k}{\varepsilon}$, where ζ is a normally distributed random number, \tilde{u}' is the r.m.s of air velocity

f l u c t u a t i o n s ,

k is the turbulent kinetic energy and ε the turbulent diffusivity.

Coupling between the dispersed (rain) and the continuous (air) phase may also be taken into consideration by calculating the momentum exchange between the two phases and alternating the air and particle trajectory calculations.

The droplets are "trapped" on the building zone, trajectory calculations are performed for all droplet sizes and the mass flow rate of particles crossing the facade (ϕ_z) and the rainfall intensity on every zone (of area A_z) are then calculated $R_z = \frac{3600 * \phi_z}{A_z}$ (mm/hr).

Local intensity factors (LIF 's) are afterwards estimated by reporting the rainfall intensity on each building zone to the undisturbed rainfall intensity: $LIF_z = \frac{R_z}{R_0}$

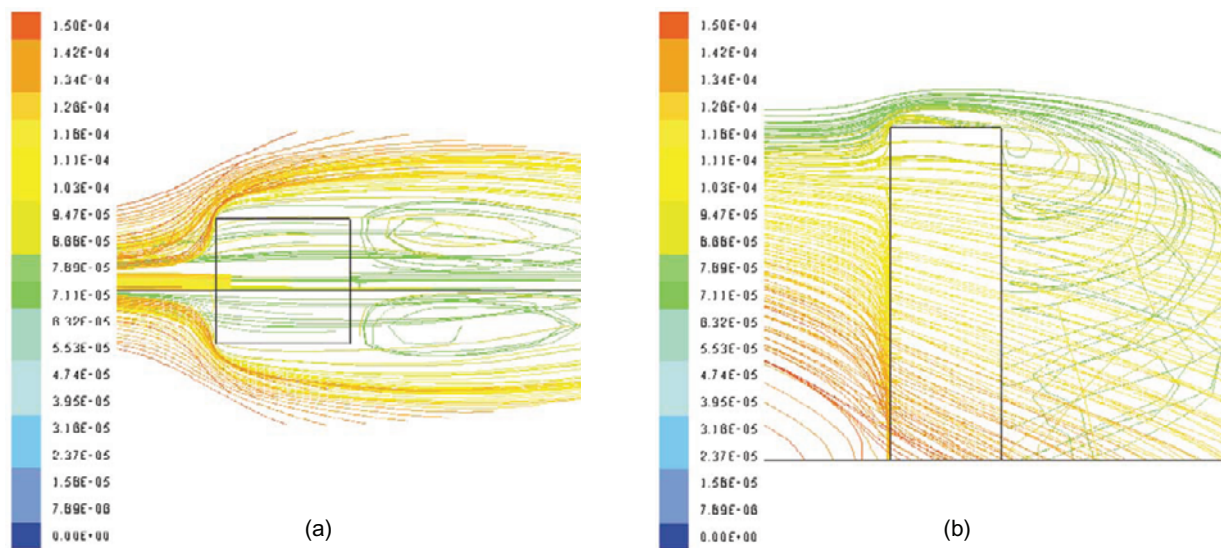


Fig. 1. Particle trajectories coloured by particle diameters-High building-
(a) horizontal plane, (b) vertical plane

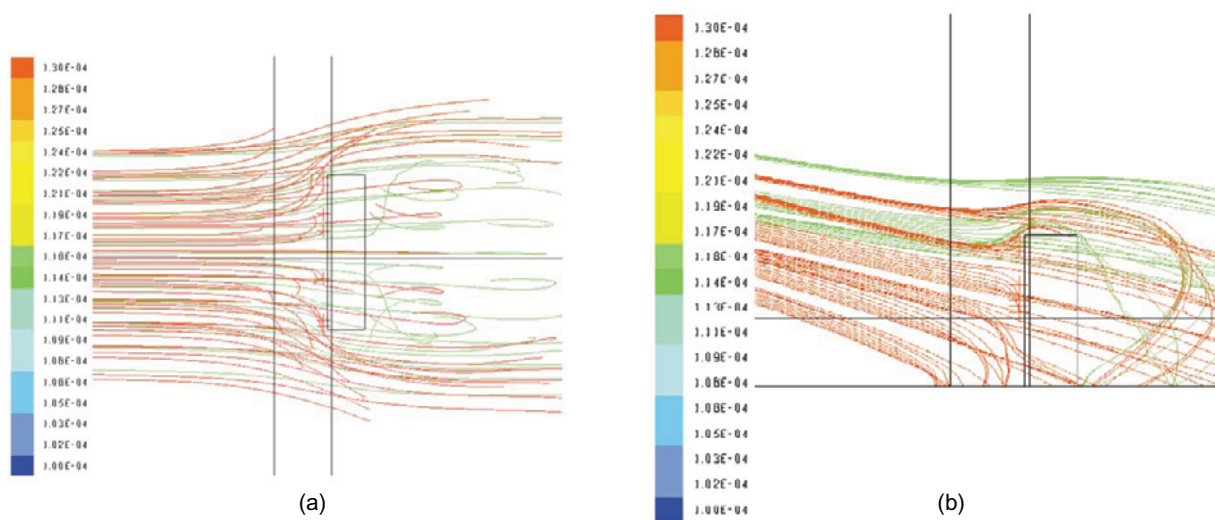


Fig. 2. Particle trajectories coloured by particle diameters-Low building-
(a) horizontal plane, (b) vertical plane

3. Comparison With Wind Tunnel Tests

The methodology described in paragraph 2 was applied in conjunction with an experiment of wetting on generic building facades previously performed by Incullet and Surry (1995) at the BLWTL. The numerical simulation reproduces closely the wind tunnel experiment, in which water was sprayed through a matrix of nine nozzles. The wind (gradient velocity, mean and turbulent velocity profiles) and the rain parameters (droplet diameter distribution, injection points, mass flow rates and undisturbed rainfall intensity) have been matched with the wind tunnel simulations. The scope of this preliminary study has been to calibrate the CFD model on simple, generic configurations which can be easily controlled.

The simulation has been performed on a structured grid, refined in regions with intense Reynolds stresses gradients. A classical $k - \epsilon$ model has been employed for the lower building and a Reynolds Stress Model for the higher building. Coupling between the two phases has been used for the high rise building. Figures. 1 and 2 present raindrop trajectories (coloured by particle diameter : red for the largest and blue for the smallest particles) for the two generic buildings. The LIF 's for the two type of buildings are compared in Fig. 3 for which the upstream velocity is $U_{\infty}=1.9$ m/s with a mean velocity profile power law $\alpha=0.28$ for both numerical and physical simulations.

Results for the higher building are also compared with results on a similar geometry which are inferred from Choi (1993). The results of the present study, see also Hangan (1998), are situated between the experimental and Choi's CFD results. Some discrepancies are observed mostly for the upper zone of the higher building and the middle zone of the lower building. However, the results show similar wetting pattern on both buildings and demonstrate that CFD wind-rain simulations can become a useful tool for wind engineers and practitioners.

CFD	EXP.	Choi(CFD)	CFD	Avg.=0.41
1.6	2.7	1.2	0.43	0.5
1.2	1.7	0.8	0.26	0.37
0.8	1.2	0.7	0.43	0.37
0.3	0.7	0.5	0.22	0.33
			EXP.	Avg.=0.46
			0.68	0.68
			0.11	0.26
			0.13	0.41
			0.29	0.29

Ro=9mm/hr Ro=10mm/hr Ro=15mm/hr

Fig. 3. *LIF*'s on facades of two generic buildings (tall building, aspect ratio 3.3:1:1 and low-rise building, aspect ratio 3.3:4.5:1)-CFD & Experiment

4. Applications

4.1 Cornice Effect for a Low-rise Building

The aim of this study is to estimate the effectiveness of the cornice design in reducing the rain impact rate on the upper part of a low rise building facade. Based on previous climatic studies at the BLWTL the wind speed and direction as well as the undisturbed rain intensity were estimated for a 10 year return period. The wind was assumed coming from South (perpendicular to the main facade of the building) with a speed $U_{10} = 10$ m/s at 10 m height and the rainfall rate was assumed to be $R_0 = 11$ mm/hr.

The building geometry is complicated but symmetrical and so symmetry boundary conditions are applied. In order to assess the effect of the cornice two simulations are performed: one without cornice and one with cornice. Figure 4 presents a detail of the building on which both wind flow and raindrop trajectories are overlaid showing typical patterns.

The building zones (areas) on which the rain impact has been considered are shown in Fig. 5. These zones cover the entire facade and the roof of the building. Both the geometry-topology generation process and the numerical grid generation emphasizes the area adjacent to the cornice zone. The cornice itself is constituted in two main parts: the canopy above the balcony 1 (left hand side in Fig. 4 and Fig. 5) and the rest of the cornice all along the building facade.

The results are analyzed for the two cases, without cornice and with cornice in terms of Local Intensity Factors (*LIF*).

Without cornice: The *LIF*'s indicate that the areas which are likely to be affected without the cornice ($LIF > 1$, Fig. 5a) are in the wake of the mechanical penthouse ($LIF = 4.3$) the frontal and inclined walls of the same mechanical block (LIF 's = 1.6 and 1.5 respectively), the balcony 1 back wall (left side, $LIF = 1.9$) and the upper wall zone (immediate below the cornice, $LIF = 1.1$).

Cornice effect: *F_j* factors have been defined as ratios (for every zone) between the *LIF*'s without and with cornice:

$$F_j = \frac{(LIF_j) \text{ without cornice}}{(LIF_j) \text{ with cornice}}$$

These factors are useful in determining the effect of the cornice for every zone: for $F_j > 1$ the cornice reduces the rainfall rate on that specific area and for $F_j < 1$ the cornice is increasing the rainfall rate to that specific area.

These factors should be reviewed along with the *LIF* factors, as increases or reductions are most significant where *LIF* values are large. It has been observed that the cornice has a positive effect (reducing the rainfall rate) for the great majority of the building zones, see Fig. 5b.

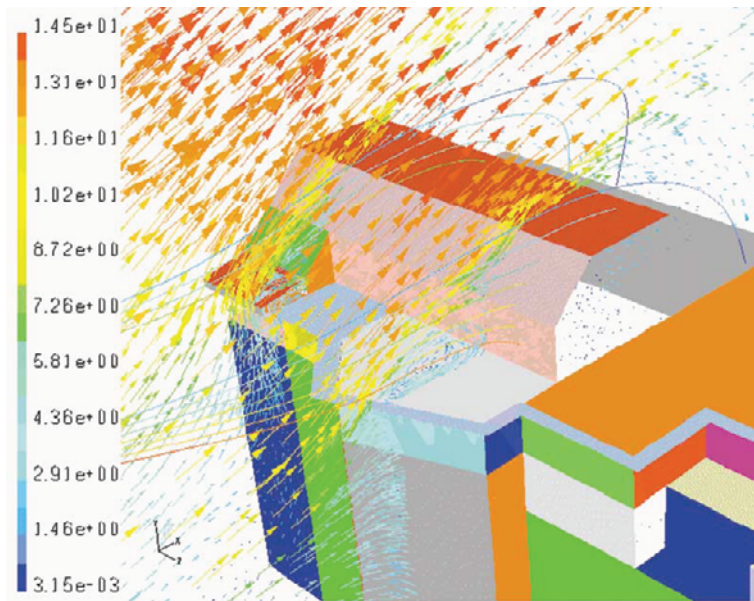


Fig. 4. Cornice zone, Airflow flow (represented by vector magnitude and colour) and raindrop trajectories (different drop sizes represented by continuous curves from two injection points)

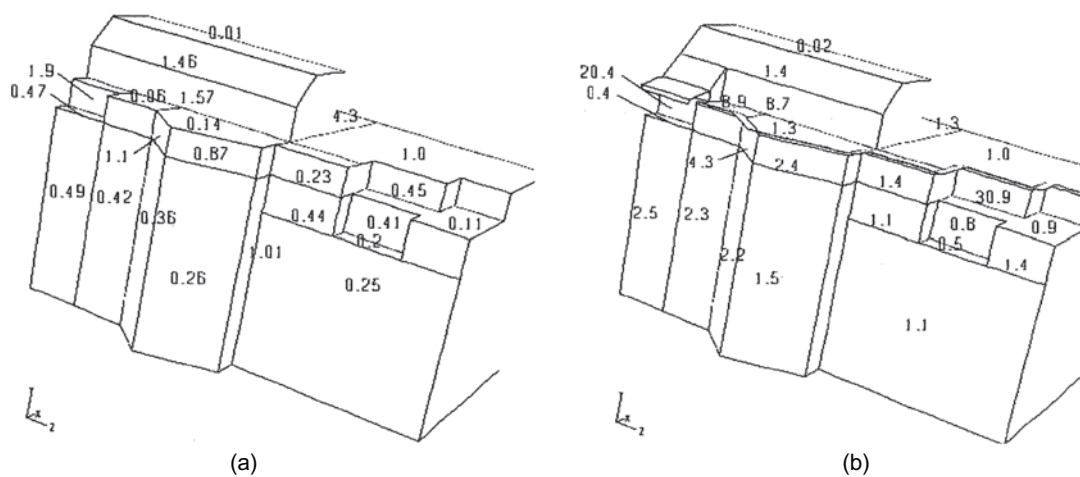


Fig. 5 (a) *LIF*'s for building zones without cornice, (b) Cornice effectiveness factors (*Fj*'s).

Reductions with a factor between 1.1 and 2.5 are expected for the main wall zones. The upper wall zones, immediate below the cornice, are well protected (*Fj* factors between 1.4 and 4.3). The back wall corresponding to balcony 1 (under the canopy, $Fj=20.4$) and the terrace (right hand side, $Fj=30.9$) are also well protected by the cornice. The only increases in rainfall rates due to the cornice occur for the balcony 2 back wall (right hand side, under the terrace, $Fj=0.5$ and $Fj=0.8$), the mechanical penthouse roof and the floor of the balcony 1 (under the canopy, $Fj=0.4$). The corresponding values of the *LIF*'s show that the only zone which is likely to be negatively affected ($LIF>1$) by the cornice is the floor of balcony 1 for which $LIF=1.11$. However, this value is considered to be acceptable in the context of the overall positive effect of the cornice.

4.2 Rainfall Drainage for a High-rise Building

This study is concerned with the rainfall drainage for a 70 degree sloping roof of a high-rise building, see Fig. 6. The steep slope overlooks a plaza area at the base of the building and this raised concerns related to the design of the gutter system, see Hangan et al. (1997).

The building is situated in a storm area characterized by heavy rains during storms. Gathering the simultaneously wind speed, wind direction and rainfall data proved to be a difficult process. A simplified approach has been taken and the calculations have been based on a 5 (five) minute event, 2 (two) year return period pluviometric record which corresponds to an undisturbed rainfall rate of $R_0=134\text{mm/hr}$ for two wind velocities ($U_{10} = 5\text{m/s}$ and $U_{10} = 10\text{m/s}$) at 10 m height in suburban terrain.

Based on numerical simulation and on previous experiments conducted at the BLWTL estimates of the Local Intensity Factors (*LIF's*) have been inferred and are presented in Fig. 7a and 7b for the two wind velocities.

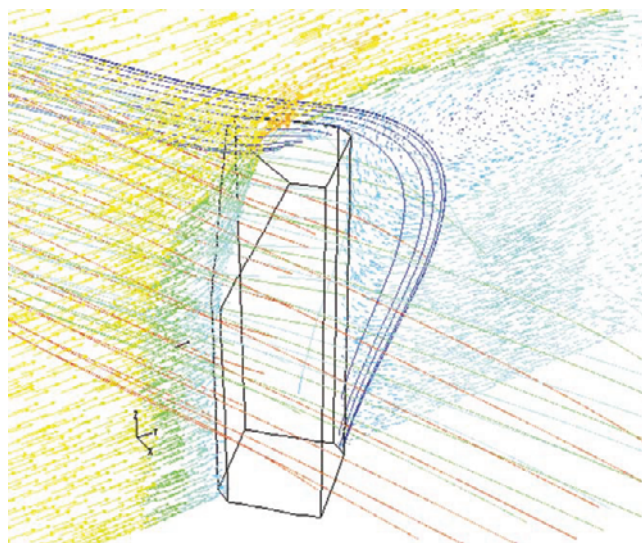


Fig. 6. Geometry, airflow and raindrop trajectories (continuous curves), high-rise building.

It is observed that the wetting on the inclined face is not uniform, with more wetting occurring at the top of the building and the corners. A strong increase in *LIF* values is observed with increased wind speed, the estimated averages are $LIF = 2$ for $U_{10} = 5\text{m/s}$ and $LIF=6$ for $U_{10} = 10\text{m/s}$.

These amplifications (*LIF's*) are for a constant rain intensity. In actual fact, the rain intensity varies with the wind speed. For tropical storm systems the maximum rainfall intensity is correlated with the maximum wind speed. However, for extra-tropical storm systems the rain intensity reduces as wind speed decreases. This offsets the amplification, and actual amplification may well be less. Other studies, see Choi (1993) suggests that the amplified wetting by wind-driven rain may be typically 1.5 over that occurring with no wind. This value was determined for wind-driven rain blowing perpendicularly to a vertical surface. In this study the 1.5 value has been adopted also for the inclined surface gutter design input in recognition that there is a trade off between the higher *LIF's* associated with the inclined surface and the lower *LIF's* associated with all wind cases that are not normal to the inclined facade. This is indicative of the uncertainty of the estimation process in the absence of detailed climatic data.

Using an amplification of 1.5 produces a flow rate on the inclined face of about 200 mm/hr. The horizontal projected area of the inclined facade is 526.5m^2 . For the suggested rainfall rate of 200 mm/hr this implies that the total flow rate generated from the roof is about 30 litres/sec. This information is important for the gutter design.

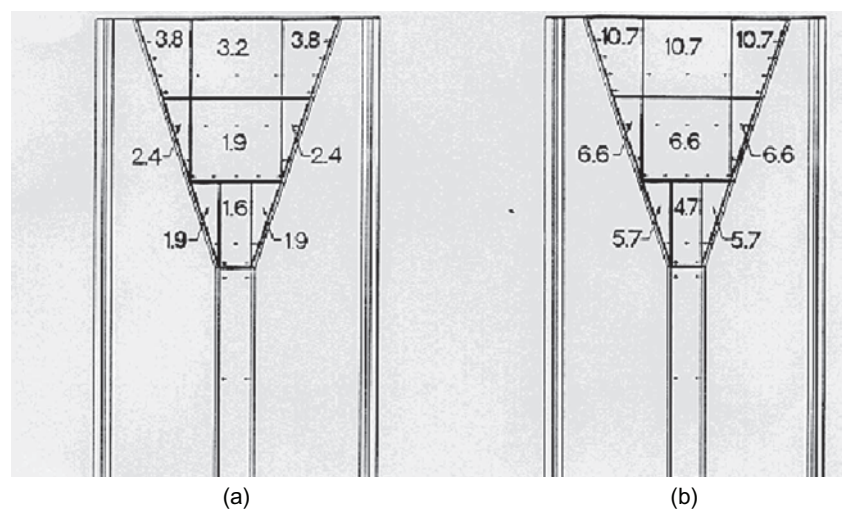


Fig. 7 Wetting distribution (LIF's) on the sloped face for $U_{10} = 5\text{m/s}$ (a) and $U_{10} = 10\text{m/s}$ (b)

5. Conclusions

Wind driven rain studies help solving problems such as precipitation protection, drainage, sealing and water disposal and CFD will probably play an important role in these studies. A numeric methodology is defined and used to simulate the wind-driven rain impact on buildings. Calibration of the numerical model versus experiment is a necessary step which ensures the reliability of the methodology. The model is applied to practical, civil engineering studies.

Further calibrations of the model are needed and comparison to full scale measurements is sought for the near future.

Acknowledgments

The work has been sponsored by the University of Western Ontario Vice-President Grant No. R2811A02 and by the Canada Mortgage and Housing Corporation.

References

- Best, A.C., The size distribution of raindrops, J. of the Royal Met. Society, Vol. 76 (1950)
- Choi, E.C.C., Simulation of Wind-Driven Rain around a Building, Journal of Wind Eng. and Ind. Aerodynamics, Vol. 46-47, (1993)
- FLUENT Inc., Users Guide (1996)
- Hangan H., CFD versus Experiment for Wind-Driven Rain Impact on Buildings, Proceedings of the 12th ASCE Engineering Mechanics Conference, LaJolla, California (1998)
- Hangan, H., Surry, D., Isyumov, N., Mikitiuk, M. and Inculet, D., A Study of Wind-driven Rain Effects for the CENU, Final Report, BLWT-SS24-(1997)
- Inculet, D. and Surry, D., Simulation of Wind-driven Rain and Wetting Patterns on Buildings, Final Report, BLWTL-CMHC, (1995)

Authors' Profiles



Horia Hangan: He received his Diplomat Engineer Degree in Aerospace Studies in 1985 from the Polytechnic University of Bucharest and his Ph.D. in Wind Engineering in 1996 from the University of Western Ontario. Before starting his Ph.D. he acted as a Research Associate at the Aviation Institute in Bucharest, Romania and as a Research Assistant at the Ecole Polytechnique Federale de Lausanne, Switzerland. After his Ph.D. he was a postdoctoral Fellow in the Laboratoire d'Etudes Aerodynamiques, Universite de Poitiers in France and he returned to the Boundary Layer Wind Tunnel Laboratory at the University of Western Ontario as an Assistant Professor. His research interests span from experimental fluid dynamics: coherent structures in wakes and jets via wavelet analysis, proper orthogonal decomposition and pattern recognition to computational fluid dynamics: multiphase/particle flows, atmospheric dispersion and internal flow studies.